

# MG-63 human osteosarcoma cells grown in monolayer and as three-dimensional tumor spheroids present a different metabolic profile: a $^1\text{H}$ NMR study

Maria Teresa Santini<sup>a,b,\*</sup>, Gabriella Rainaldi<sup>a,b</sup>, Rocco Romano<sup>b,c</sup>, Antonella Ferrante<sup>a</sup>, Stefania Clemente<sup>c</sup>, Andrea Motta<sup>b,d</sup>, Pietro Luigi Indovina<sup>b,c</sup>

<sup>a</sup>Dipartimento di Tecnologie e Salute, Istituto Superiore di Sanità, Viale Regina Elena 299, 00161 Rome, Italy

<sup>b</sup>Istituto Nazionale per la Fisica della Materia, Unità di Napoli, Complesso Universitario Monte S. Angelo, Via Cinthia, 80126 Naples, Italy

<sup>c</sup>Dipartimento di Scienze Fisiche, Università di Napoli 'Federico II', Complesso Universitario Monte S. Angelo, Via Cinthia, 80126 Naples, Italy

<sup>d</sup>Consiglio Nazionale delle Ricerche (C.N.R.), Istituto di Chimica Biomolecolare, Comprensorio A. Olivetti, Edificio 70, Via Campi Flegrei 34, 80078 Pozzuoli, Naples, Italy

Received 16 October 2003; revised 18 November 2003; accepted 2 December 2003

First published online 18 December 2003

Edited by Veli-Pekka Lehto

**Abstract** High resolution proton nuclear magnetic resonance ( $^1\text{H}$  NMR) spectroscopy was used to determine if the same cell line (MG-63 human osteosarcoma cells) grown in monolayer or as small (about 50–80  $\mu\text{m}$  in diameter), three-dimensional tumor spheroids with no hypoxic center has different metabolic characteristics. Consequently, the  $^1\text{H}$  NMR spectra were obtained from both types of cultures and then compared. The results indicate that the type of cellular spatial array determines specific changes in MG-63 cells. In particular, small but significant differences in lactate and alanine indicating a perturbation in energy metabolism were observed in the two cell models. In addition, although variations in  $\text{CH}_2$  and  $\text{CH}_3$  groups were also seen, it is not possible at this time to establish if lipid metabolism is truly different in cells and spheroids.

© 2003 Federation of European Biochemical Societies. Published by Elsevier B.V. All rights reserved.

**Key words:** High resolution nuclear magnetic resonance spectroscopy; Human osteosarcoma cell; Three-dimensional tumor spheroid; Monolayer culture

## 1. Introduction

Two- and three-dimensional in vitro cultures of tumor cells have yielded much valuable information regarding various aspects of tumor cell biology. In particular, monolayer cultures have provided a deeper understanding principally of the underlying cellular mechanisms responsible for tumor cell behavior while three-dimensional ones (i.e. multicellular spheroids) have permitted the study of cell–cell interactions in a context more closely resembling tumor tissue architecture [1–3]. It is apparent that the knowledge obtained from these two cell culture systems with such different cellular organizations is complementary and that the study of both can give a more comprehensive view of tumor cell biology as a whole. How-

ever, the information that emerges must be compared and integrated in order to be better comprehended.

High resolution nuclear magnetic resonance (NMR) spectroscopy is an extremely useful tool in examining, non-invasively, tumor cells grown both in monolayer and as three-dimensional spheroids. For example, this technique has been applied to examining tumor cell growth [4], membrane lipid metabolism [5], efficacy of various treatments [6] and cholesterol metabolism [7] in monolayer cultures as well as metabolism [8] and response to anti-neoplastic agents [9] in three-dimensional tumor spheroids. Because of their particular structure, proton NMR ( $^1\text{H}$  NMR) can also be used to study spheroid morphology by micro-imaging [10]. As can be discerned from a careful analysis of these and other papers which use NMR, much important information regarding cell function and cellular organization can be obtained by this technique. However, as is also apparent, few attempts have been made to compare and integrate the complementary information which emerges from monolayer and spheroid cultures.

It was the purpose of the present paper to attempt to compare monolayer and spheroid cultures of the same cell type (MG-63 human osteosarcoma cells) in order to determine if the spatial organization of cells (two- and three-dimensional architecture) can induce significant variations. For this task, high resolution  $^1\text{H}$  NMR spectra were obtained from both types of cultures and then compared by utilizing a new algorithm developed by our group. In order to make certain that the differences observed were not due to the effects of hypoxia, small spheroids (about 50–80  $\mu\text{m}$  in diameter) with no hypoxic center were used. In addition, in order to exclude the effects of cell growth, cells from both monolayer and spheroid cultures were examined for their growth characteristics (cell cycle analysis) and collected when these were very similar. Apoptosis was also checked and found to be very low (< 2%). The results seem to indicate that the type of spatial array determines specific changes in cell function. In particular, small but significant differences in lactate and alanine indicating a perturbation in energy metabolism were observed in the two cell models. In addition, although variations in  $\text{CH}_2$  and  $\text{CH}_3$  groups were also seen, it is not possible at this time to establish if lipid metabolism is truly different in cells and spheroids.

\*Corresponding author. Fax: (39)-06-49387140.  
E-mail address: [santini@iss.it](mailto:santini@iss.it) (M.T. Santini).

## 2. Materials and methods

### 2.1. Monolayer cells

MG-63 cells (a human osteosarcoma cell line) purchased from the Istituto Zooprofilattico Sperimentale della Lombardia e dell'Emilia (Brescia, Italy) were grown in monolayer in tissue culture flasks (Nunc A/S, Roskilde, Denmark) containing RPMI 1640 (Gibco BRL, Burlington, ON, Canada) supplemented with 10% heat-inactivated fetal bovine serum (FBS Characterized; Hyclone, Logan, UT, USA), non-essential amino acids, 100 IU/ml penicillin and 100 µg/ml streptomycin and incubated at 37°C in a 5% CO<sub>2</sub> atmosphere. Monolayer cells were collected at 48 h of growth.

### 2.2. Multicellular tumor spheroids

MG-63 cells were grown in monolayer as described above and detached from the substratum using 10 mM EDTA (pH 7.4) and 0.25% trypsin. The cells ( $5.0 \times 10^5$  cells/well) were then seeded on 3% agar dissolved in complete medium in six well tissue culture plates (Nunc). Spheroids were collected from the growth medium at 48 h of growth when their diameters were in the range of 50–80 µm, determined as described below.

### 2.3. Characterization of monolayer cells and multicellular tumor spheroids

**2.3.1. Light microscopy.** MG-63 monolayer cells and spheroids were observed and photographed in the tissue culture flasks and plates, respectively, using an inverted Zeiss Axiovert light microscope. The diameter of the spheroids was determined using an ocular reticule and found to be in the range of 50–80 µm.

**2.3.2. Scanning electron microscopy.** Monolayer cells and spheroids were fixed with 2.5% glutaraldehyde, post-fixed in 1% osmium tetroxide, dehydrated through graded ethanols, critical point dried in CO<sub>2</sub>, gold coated by sputtering and examined with a Cambridge 360 scanning electron microscope. It was noted that fixed spheroids had shrunk by about 10% when compared to those freshly harvested.

**2.3.3. Paraffin-embedded sections of spheroids for light microscopy.** Spheroids were fixed, dehydrated and embedded in paraffin. Sections were obtained with an ultramicrotome (LKB, Nova). In order to investigate the organization of nuclear chromatin, sections were deparaffinized, stained utilizing 1 µg/ml of the chromatin stain Hoechst 33258 (Sigma Chemicals, St. Louis, MO, USA) and photographed with a Zeiss Axiovert fluorescence microscope. The percentage of necrotic and apoptotic cells obtained in MG-63 spheroids was determined by counting at high magnification (500×) at least 500 cells of each sample in randomly selected areas. In particular, in order to distinguish apoptotic and necrotic cells, the nuclear morphological and ultrastructural parameters typical of these two kinds of cell death previously described were taken into account [11–13]. Specifically, cells whose nuclei had a uniform and homogeneous distribution of uncondensed chromatin were considered normal. Cells having clumped or condensed nuclear chromatin and/or chromatin marginalized under the nuclear membrane were considered apoptotic. Finally, cells whose nuclei presented shrunken and/or disintegrated chromatin were considered necrotic.

### 2.4. Cell cycle analysis

For monolayer cells, the single-cell suspension was obtained as described above while for MG-63 spheroids it was first necessary to disaggregate the spheroids by gentle pipetting. Both single-cell suspensions obtained from monolayer cells and those from spheroids were fixed in ice-cold 70% ethanol and incubated in phosphate-buffered saline (PBS) containing 50 µg/ml of the DNA fluorescent probe propidium iodide. Fluorescence was analyzed with a FACScan flow cytometer (Becton Dickinson, Mountain View, CA, USA) equipped with a 15 mW, 488 nm, air-cooled argon ion laser. Analysis was conducted using the Sfit model in the CellFit® software (Becton Dickinson).

### 2.5. Preparation of perchloric acid extracts of MG-63 cells and spheroids

Cells and spheroids were collected and placed immediately on ice and then washed with cold PBS (pH 7.2). To the pellet was added a cold 30% perchloric acid solution (equal to twice the pellet volume). The perchloric acid was neutralized by adding K<sub>2</sub>CO<sub>3</sub> until a pH of about 7.4 was reached. The solution was centrifuged, the supernatant removed and stored at –80°C for about 2 h and then lyophilized

overnight at –50°C. The samples were stored at –20°C until NMR measurement.

### 2.6. High resolution <sup>1</sup>H NMR measurements of whole cells and extracts

Monolayer cells and whole spheroids (about 10<sup>8</sup> cells) were collected, washed in PBS and resuspended in 1.0 ml of the same buffer with 10 µl of a 10% TSP (sodium 3-trimethylsilyl[2,2,3,3-D<sub>4</sub>]propionate) solution used as internal standard. High resolution <sup>1</sup>H NMR spectra were obtained on a Bruker DRX-500 spectrometer operating at 500 MHz. The measurements were performed at a probe temperature of 300 K in the presence of about 15% of deuterium oxide used as a lock signal. The <sup>1</sup>H free induction decays (FIDs) of the cells were obtained with a 9 µs pulse (90° flip angle), a ±4006.4 Hz (±8 ppm) spectral window and 8000 data points. The relaxation delay between scans was set to 5.0 s, and the acquisition time was 1.2 s. Therefore the recycling time of the experiment was 6.2 s. Intensity of the water signal was reduced by the WATERGATE field gradient-based sequence [14]. Each spectrum represented the sum of 128 FIDs. The measured FIDs were zero-filled to 64 K and Fourier transformed without apodization to the frequency domain. The spectra were manually phase-corrected (0th and 1st order) and finally a spline function baseline correction was applied. Resonance chemical shifts were expressed in ppm with reference to the internal standard TSP assigned to 0 ppm [15,16]. Spectral lines were analyzed by fitting them with Lorentzian shape lines (the MacFID 5.5 program was used). All measurements were repeated at least five times using five different spheroid preparations.

For the perchloric acid extract measurements, the stored lyophilized powder was resuspended in D<sub>2</sub>O and the pH was adjusted to about 7.1 with DCI or NaOD and 4 ml of a 10% TSP solution was added. The high resolution <sup>1</sup>H NMR spectra were also obtained at 300 K on the same Bruker DRX-500 spectrometer operating at 500 MHz. The residual water resonance was reduced by pre-saturating the signal with a low power pulse for 1 s before acquisition using standard Bruker software. Two hundred and fifty-six transients of 16000 points, with 6024 Hz of spectral width, were acquired for each sample. The relaxation delay between scans was set to 5.0 s, and the acquisition time was 1.2 s. Therefore the recycling time of the experiment was 6.2 s. All measurements were repeated five times using five different cell extract preparations.

### 2.7. Normalization algorithm

In order to obtain relative quantitative information between whole MG-63 monolayer cells and spheroids, a comparison was conducted by normalization of the spectra using a modification of the MiRaNAI algorithm recently developed by our group [17]. It is based on the assumption that variations in signal intensities due to concentration differences result in proportional changes in the majority of spectral intensities, while non-proportional variations may most likely be attributed to intrinsic differences of the system(s) under investigation. The proportional variations are described by a normalization factor *R*, which is calculated by the MiRaNAI algorithm. This calculation is conducted by minimizing the rank of a Hankel matrix constructed with the differences in the FIDs of the two systems. Specifically, one of the FIDs is multiplied by various *R*<sub>test</sub> values until *R*<sub>test</sub> = *R*. When this is the case, the FIDs are correctly normalized and the differences do not contain the proportional signal intensities, but rather only the non-proportional part of the signal intensities. The MiRaNAI algorithm assumes that there are no differences in the resolution of the signals of the systems. However, since one has to take into account slight variations in resolution due to the different packing in spheroids and cells [18], in order to apply the MiRaNAI algorithm in the present study, the small variations in spectral resolution were modeled with an apodization constant  $\tau$ , which has to be calculated together with the normalization constant *R*. In this specific case, the Hankel rank matrix depends on the two parameters and, consequently, it is minimized by the use of the *downhill simplex method* [19,20] and the *simulated annealing method* [21–24], modified to take into account the discrete value properties of the function (mathematical details are in [25]). The spectra of cell extracts were normalized using an internal reference signal as described in [26].

### 2.8. Statistical analyses

All statistical analyses not otherwise specified were carried out using the paired Student's *t*-test.

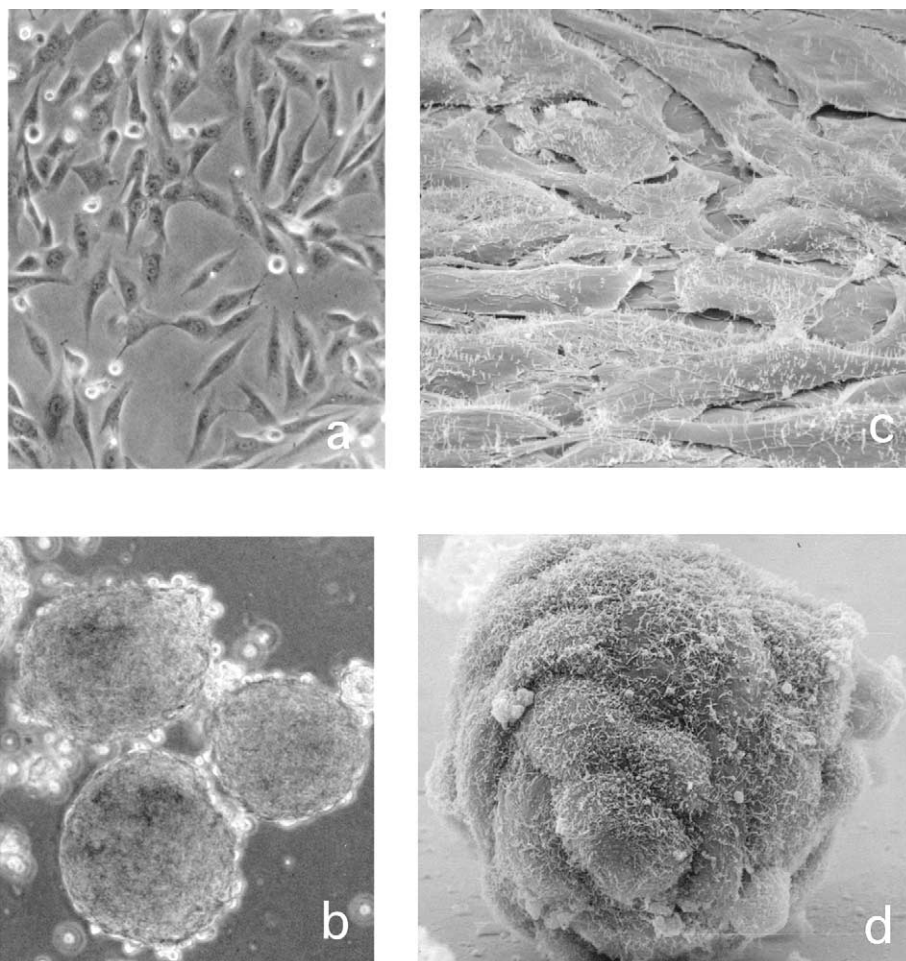


Fig. 1. Light micrographs (a,b) and scanning electron micrographs (c,d) of MG-63 osteosarcoma cells grown in monolayer (a,c) and as three-dimensional tumor spheroids (b,d) after 48 h of growth. As can be seen, monolayer cells are polygonal in shape and well-separated from each other while spheroids appear as round masses of cells in which individual cells can hardly be recognized. Microvilli are present on the surfaces of both monolayer cells and spheroids. (Magnification for light micrographs:  $\times 360$ ; magnification for scanning electron micrographs:  $\times 900$ .)

### 3. Results

#### 3.1. Characterization of monolayer cells and multicellular tumor spheroids

**3.1.1. Light and scanning electron microscopy.** As can be seen in Fig. 1, both light microscopy (a,b) and scanning electron microscopy (c,d) demonstrate that MG-63 osteosarcoma cells grown in monolayer are very different from the same cells grown as three-dimensional spheroids. In fact, monolayer cells (a,c) are flat, well-separated from each other and polygonal in shape. By contrast, in spheroids, single cells have completely lost their polygonal shape and cannot be clearly distinguished from each other due to their compaction and three-dimensional architecture. In addition, it should be noted that numerous microvilli can be observed on the cell surface of both monolayer cells (c) and spheroids (d).

**3.1.2. Paraffin-embedded sections of spheroids.** In order to examine the internal organization of whole MG-63 spheroids as well as to determine apoptosis and necrosis, paraffin-embedded sections stained with the chromatin dye Hoechst were prepared. As can be seen in Fig. 2, no necrotic center can be observed in these spheroids. In fact, mitotic cells indicative of active proliferation are often evident in the central region of the spheroids. In addition, chromatin is well-distributed in the

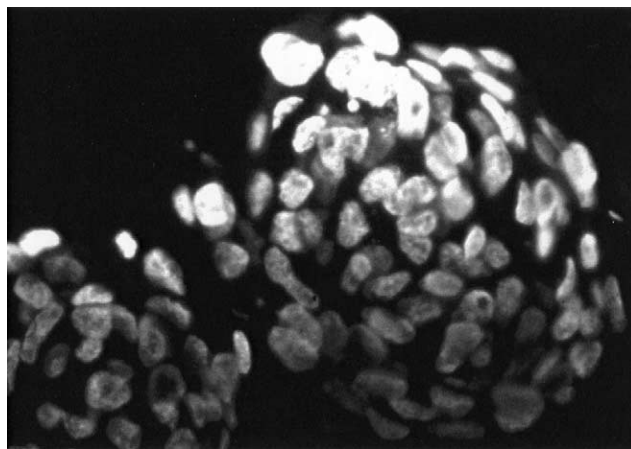


Fig. 2. Fluorescence micrograph of paraffin-embedded sections of MG-63 spheroids stained with the chromatin dye Hoechst after 48 h of growth. As can be seen, spheroids do not contain a necrotic center and the chromatin is uniformly distributed in the nuclei. In addition, cells are uniformly associated with each other. (Magnification:  $\times 670$ .)

nuclei in cells throughout the spheroid, including the center. No signs of cell damage typical of apoptotic death or necrotic death are present. Both types of death are below 2% (data not shown), values very close to those of monolayer cells.

### 3.2. Cell cycle analysis

In order to make certain that both MG-63 cells from monolayer cultures and from multicellular spheroids examined by NMR had the same cell cycle distribution, the various phases of the cell cycle were determined by cytofluorometric analyses. Cells from both monolayer and spheroid cultures have a similar cell cycle phase distribution. The  $G_0/G_1$  phase is  $60.8 \pm 1.5\%$  and  $65.9 \pm 1.8\%$ , the S phase is  $21.3 \pm 1.4\%$  and  $19.0 \pm 1.2\%$  and the  $G_2/M$  phase is  $18.1 \pm 1.1\%$  and  $15.1 \pm 1.0\%$  for monolayer and spheroids, respectively.

### 3.3. $^1H$ NMR measurements of whole cells and perchloric acid extracts

In Fig. 3 is shown one of the five 500 MHz  $^1H$  NMR experiments conducted on whole MG-63 cells grown in monolayer (a) and as spheroids (b). The spectra (in the range of 0–4.0 ppm) of monolayer and spheroid cells have the same general appearance. Nonetheless, significant differences can be noted. In order to better examine these differences, the spectra were normalized using the algorithm described above and the normalized spectrum of monolayer MG-63 cells was subtracted from the normalized spectrum of spheroids. The re-

sulting difference spectrum is shown in Fig. 3c. As can be seen, in the difference spectrum, intense peaks, indicating variations between MG-63 cells grown in monolayer and as spheroids, can be observed. Of particular interest are the signals resonating at about 3.2 ppm (choline-containing metabolites, Cho including choline, phosphocholine and glycerophosphocholine), 1.48 ppm (alanine, Ala), 1.33 ppm (lactate, Lac) and 0.9–1.3 ppm ( $CH_2$  and  $CH_3$  groups arising from fatty acyl chains of lipids). After the normalization procedure described above, these signals, which showed important qualitative variations, were simulated in order to obtain more quantitative information [27]. The differences in peak area percentages [(spheroid peak—monolayer peak)/spheroid peak  $\times 100$ ] were evaluated using the Bienayme–Tshebycheff hypothesis test [28,29] that is suitable for small sample numbers (number of sample points  $< 20$ ) and independent of the distribution function. In the histogram are summarized the most significant variations observed between MG-63 cells grown in monolayer and spheroids in the five separate experiments conducted. The means and standard deviations of these five experiments are presented. The differences were considered significant ( $P < 0.05$ ). As can be seen in this histogram, statistically significant decreases are seen in alanine, lactate and  $CH_3$  lipids in spheroids with respect to monolayer cultures. A significant increase in  $CH_2$  lipids is also seen in spheroids. Variations in choline-containing metabolites were statistically not significant and therefore will not be discussed further.

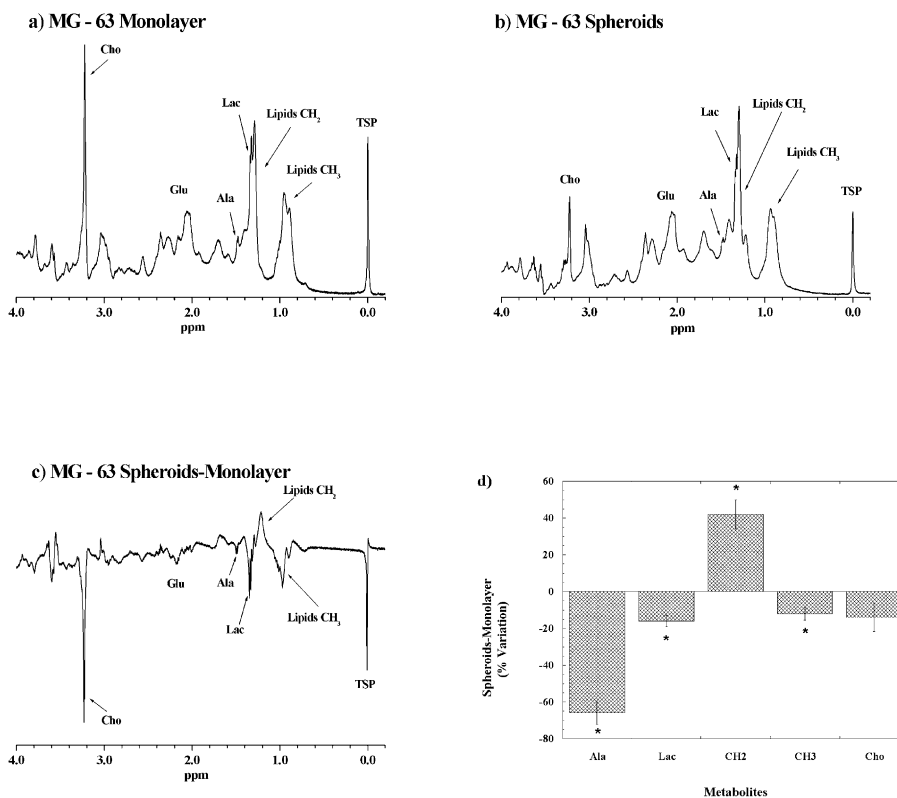


Fig. 3. Representative high resolution 500 MHz  $^1H$  NMR spectra in the range of 0–4 ppm of whole MG-63 cells grown (a) in monolayer and (b) as spheroids after 48 h of growth. c: The resulting difference spectrum (spheroids—monolayer/spheroids). Only the metabolites in which important differences were observed are assigned. Abbreviations: Cho, choline-containing metabolites; Ala, alanine; Lac, lactate;  $CH_2$  lipids,  $CH_2$  chains of lipid fatty acids;  $CH_3$  lipids,  $CH_3$  chains of lipid fatty acids; and TSP, standard. The histogram in panel d shows the variations of each metabolite in percent. The means and standard deviations of five separate experiments are shown. Asterisks indicate significant changes ( $P < 0.05$ ). The quantitative data presented were obtained after simulation as described in the text. Positive values indicate the increased presence of the metabolite in spheroids.

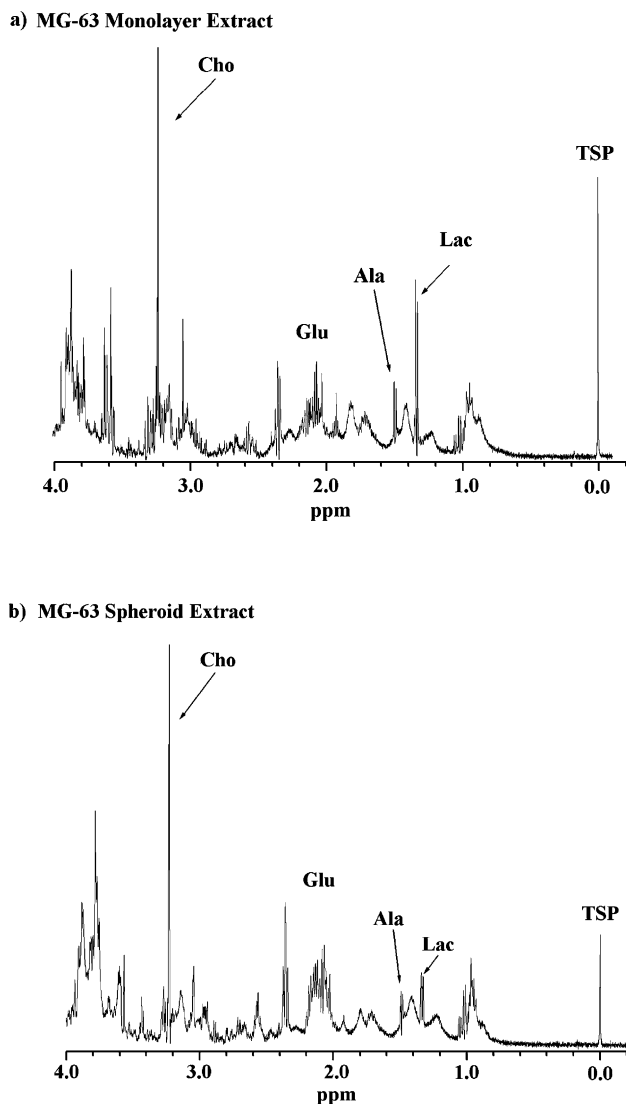


Fig. 4. Representative high resolution 500 MHz  $^1\text{H}$  NMR spectra in the range of 0–4 ppm of extracts of MG-63 cells grown (a) in monolayer and (b) as spheroids after 48 h of growth. The abbreviations are the same as in Fig. 3.

In Fig. 4 is shown one of the five 500 MHz  $^1\text{H}$  NMR experiments conducted on extracts of MG-63 cells grown in monolayer (a) and as spheroids (b). The means and standard deviations of the five extract experiments conducted confirm the data obtained with whole cells in the soluble metabolites alanine and lactate. Significant decreases in alanine ( $-6.9\% \pm 3.0\%$ ) and lactate ( $-77.5\% \pm 20.0\%$ ) were seen in spheroids with respect to monolayer cells.

#### 4. Discussion

Three-dimensional tumor spheroids conserve many of the characteristics of early, avascular solid tumors and thus represent a useful *in vitro* model system to investigate many aspects of tumor biology. Because of their specific cell–cell and cell–matrix interactions, growth characteristics, nutrient and oxygen diffusion dynamics and the existence of heterogeneous microregions, these systems reproduce *in vivo* solid tumors much more closely. In addition, the use of cell lines to

produce them makes spheroids highly standardized models which are extremely well-suited for fundamental studies in tumor cell biology. Numerous studies have been conducted on multicellular tumor spheroids using NMR spectroscopy. For instance,  $^1\text{H}$  NMR has been utilized to obtain images at the microscopic level of EMT6/Ro and HT1080 three-dimensional spheroids [10]. In this study, the morphology of the spheroids, including the necrotic center, is well-documented.  $^1\text{H}$  NMR and magnetic resonance imaging have also been used to study the morphology of V79 lung tumor spheroids [30]. In this paper, differences in the characteristics of the spectra obtained from the viable rim and central necrotic area were demonstrated. Phosphorus NMR was used in another work to examine the lipid metabolism of T47D human breast cancer spheroids [31]. In this report, it was found that phosphomonoester lipid precursors vary as a function of spheroid size. This information is extremely useful since phosphomonoester precursors have often been associated with the response of chemotherapeutic treatments. Thus, although much valuable information has been obtained using spheroids, few studies have concentrated their efforts in comparing quantitatively the data gathered from these systems to those from monolayer cultures.

One reason that the NMR spectra of monolayer and spheroid cultures have not been compared is that it is not so easy to accomplish this task. For instance, significant differences in spectral resolution and, consequently, line-broadening can render a quantitative comparison difficult. Therefore, in the present paper, an algorithm to compare quantitatively the NMR spectra of these two types of cell systems was designed and applied to MG-63 cells. For the first time in the literature, at least to our knowledge, a quantitative comparison of the spectra of MG-63 monolayer cultures and spheroids was conducted. However, before discussing the differences found, it should be pointed out that the spectra of both MG-63 cells grown in monolayer or as spheroids are well-resolved and are very similar to each other. The most evident difference is in the spectral resolution of monolayer cells and spheroids. Similar variations in resolution of the spectra of the two cell models were also observed by other investigators [18]. A more careful analysis and quantitative comparison of the spectra utilizing the algorithm developed revealed that important differences exist in MG-63 cells if they are grown in monolayer or as three-dimensional tumor spheroids. The variations observed may be grouped into two main categories: those related to alterations in lipid metabolism ( $\text{CH}_2$  and  $\text{CH}_3$  lipids) and those related to perturbations in cell energy metabolism (alanine and lactate).

Variations in what are often called mobile lipids, i.e. the spectral peaks resonating at about 0.9 and 1.3 ppm arising from methyl and methylene groups of fatty acyl chains of lipids, respectively [32–34], were found between MG-63 cells grown in monolayer and as three-dimensional spheroids. The methyl and methylene mobile lipid resonances are especially important since these have been associated directly with transformed cells and have often been considered markers of the tumor state itself [35,36]. It should also be noted that these resonances have additional contributions from neutral amino acid methyl and methylene groups such as valine, leucine and isoleucine and that the changes observed in this paper may be strongly influenced by these contributions. Therefore, in whole cells, the variations noted may be the result of both

lipids and amino acids while perchloric acid extracts are not completely suitable for extraction of lipids. Consequently, from the data reported, it cannot be concluded whether lipid metabolism is different in the two cell models examined. Further studies are necessary.

Three-dimensional growth also appears to induce small variations in the bioenergetics of MG-63 cells. The decrease observed in alanine and lactate in spheroids in both whole cell studies and cell extracts may indicate alterations, albeit subtle ones, in the metabolism of these three-dimensional structures when compared to cells in monolayer. It should be recalled that tumor cells produce energy by means of various complex metabolic pathways and by utilizing different substrates. For instance, both aerobic and anaerobic glycolysis can take place in these cells. In fact, although tumor cells have all the necessary enzymes to carry out normal aerobic glycolysis, anaerobic glycolysis is increased [37] and most of the glucose consumed is converted into lactate [38]. The lactate produced in this way is sometimes exported from the cell via the monocarboxylic acid transporter. If this is the case, perhaps the extrusion of lactate by this transporter is different in the two cell models leading to differences in the lactate present. On the other hand, it can also be hypothesized that spheroids contain less lactate because they produce less as a consequence of increased aerobic glycolysis. At the present time, we are unable to distinguish between these or other possible explanations for the variations in lactate observed and further experiments are necessary.

Other workers have demonstrated an increase rather than a decrease in lactate in spheroids with respect to monolayer cultures [18]. Kotitschke and co-workers showed that multicellular tumor spheroids obtained from the GaMG human glioma cell line had greater lactate accumulation than the same cells grown in monolayer. These apparently contradictory results may be explained by the fact that these investigators used spheroids after 7–10 days of growth with diameters of 300–400  $\mu\text{m}$  (most likely with a necrotic center) while in the present report proliferating, 2 day old spheroids with diameters of 50–80  $\mu\text{m}$  were utilized. Thus, it may be hypothesized that the increase in lactate observed by these other workers is probably due to the formation of lactate in the necrotic central region. In fact, an increase in lactate in this region was observed directly in another study investigating larger V79 lung tumor spheroids with both  $^1\text{H}$  NMR and micro-imaging techniques [29]. Therefore, it appears clear that small spheroids behave in a very different manner than large ones and that it is very important to define precisely the three-dimensional culture model that is being investigated. Finally, Kotitschke and co-workers [18] discussed only the extremely evident variations in lactate between monolayer cells and spheroids and did not comment on the other alterations also present in the spectra. If this was due to the fact that these other resonances could not be adequately quantified, the importance of the algorithm described in the present report is further highlighted.

In conclusion, the data presented in this report seem to suggest that the same cell line grown in monolayer and as three-dimensional spheroids can be more precisely compared if the algorithm described in this paper is used. In addition, this comparative analysis may result in variations in important metabolites between the two cell models used. Perhaps these changes are due to the diverse organization of cells in

monolayer and in spheroids in which both the metabolism of lipids and energy production is dramatically different. With these considerations in mind, the present report should be considered a pilot study for future investigations in which the metabolic differences observed between MG-63 osteosarcoma monolayer cells and spheroids will also be examined in other tumor cell types. Further experiments are already under way in our laboratory in order to determine if the metabolic variations are a general phenomenon or only specifically related to MG-63 cells.

*Acknowledgements:* The authors wish to thank Dr. P. Filippini for her technical assistance in performing the flow cytometric measurements and also the Sezione B of the Istituto Nazionale per la Fisica della Materia for the PAIS 2002 grant entitled 'Biophysical investigations of tumor cells grown in monolayer and as three-dimensional spheroids' to Prof. P.L. Indovina.

## References

- [1] Sutherland, R.M. (1988) *Science* 240, 177–184.
- [2] Durand, R.E. (1990) *Cell Tissue Kinet.* 23, 141–159.
- [3] Santini, M.T., Rainaldi, G. and Indovina, P.L. (2000) *Crit. Rev. Oncol. Hematol.* 36, 75–87.
- [4] Barba, I., Cabanas, M.E. and Arus, C. (1999) *Cancer Res.* 59, 1861–1868.
- [5] Le Moyec, L., Tatoud, R., Eugene, M., Gauville, C., Primot, I., Charlemagne, D. and Calvo, F. (1992) *Br. J. Cancer* 66, 623–628.
- [6] Cooper, W.A., Bartier, W.A., Rideout, D.C. and Delikatny, E.J. (2001) *Magn. Reson. Med.* 45, 1001–1010.
- [7] Santini, M.T., Romano, R., Rainaldi, G., Filippini, P., Bravo, E., Porcu, L., Motta, A., Calcabrini, A., Meschini, S., Indovina, P.L. and Arancia, G. (2001) *Biochim. Biophys. Acta* 1531, 111–131.
- [8] Wehrle, J.P., Ng, C.E., McGovern, K.A., Aiken, N.R., Shungu, D.C., Change, E.M. and Glickson, J.D. (2000) *NMR Biomed.* 13, 349–360.
- [9] Chen, T.B., Huzak, M., Macura, S. and Vuk-Pavlovic, S. (1994) *Cancer Lett.* 86, 41–51.
- [10] Sillerud, L.O., Freyer, J.P., Neeman, M. and Mattingly, M.A. (1990) *Magn. Reson. Med.* 16, 380–389.
- [11] Bär, P.R. (1996) *Life Sci.* 59, 369–378.
- [12] Oberhammer, F.A., Froschl, G., Tiefenbacher, R., Inayat-Hussain, S.H., Cain, K. and Stopper, H. (1996) *Microsc. Res. Tech.* 34, 247–258.
- [13] Inayat-Hussain, S.H., Cohen, G.M. and Cain, K. (1999) *Cell Biol. Toxicol.* 15, 381–387.
- [14] Píotto, M., Saudek, V. and Sklenar, V. (1992) *J. Biomol. NMR* 2, 661–665.
- [15] Mountford, C.E., Lean, C.L. and MacKinnon, W.B. (1993) *Annu. Rep. NMR Spectrosc.* 27, 173–215.
- [16] Behar, K.L. and Ogino, T. (1991) *Magn. Reson. Med.* 17, 285–303.
- [17] Romano, R., Santini, M.T. and Indovina, P.L. (2000) *J. Magn. Reson.* 146, 89–99.
- [18] Kotitschke, K., Tonn, J.C., Goldbrunner, R., Bogdahn, U. and Haase, A. (1995) *J. Magn. Reson.* 109, 39–43.
- [19] Nelder, J.A. and Mead, R. (1965) *Comput. J.* 7, 308–313.
- [20] Caceci, M.S. and Cacheris, W.P. (1984) *BYTE* 5, 340–362.
- [21] Kirkpatrick, S., Gelatt, C.D. and Vecchi, M.P. (1983) *Science* 220, 671–680.
- [22] Kirkpatrick, S. (1984) *J. Stat. Phys.* 34, 975–986.
- [23] Metropolis, N., Rosenbluth, A., Rosenbluth, M., Teller, A. and Teller, E. (1953) *J. Chem. Phys.* 21, 1087–1092.
- [24] Press, W.H., Teukolsky, S.A., Wetterling, W.T. and Flannery, B.P. (1986) *Numerical Recipes in C: The Art of Scientific Computing*, 2nd edn., Cambridge University Press, Cambridge.
- [25] Romano, R., Motta, A., Camassa, S., Pagano, C., Santini, M.T. and Indovina, P.L. (2002) *J. Magn. Reson.* 155, 226–235.
- [26] Fan, T.W.-M. (1996) *Prog. Magn. Reson.* 28, 161–219.
- [27] van den Boogart, A., Ala-Korpela, M., Jokisaari, J. and Grifiths, J.R. (1994) *Magn. Reson. Med.* 31, 347–358.
- [28] Ross, S.M. (1987) *Introduction to Probability and Statistics for Engineers and Scientists*, John Wiley and Sons, New York.

- [29] Eadie, W.T., Drijard, D., James, F.E., Ross, M. and Sadoulet, B. (1971) *Statistical Methods in Experimental Physics*, North Holland Publishing Company, Amsterdam.
- [30] Minard, K.R., Guo, X. and Wind, R.A. (1998) *J. Magn. Reson.* 133, 368–373.
- [31] Ronen, S.M., Stier, A. and Degani, H. (1990) *FEBS Lett.* 266, 147–149.
- [32] Bloom, M., Holmes, K.T., Mountford, C.E. and Williams, P.G. (1986) *J. Magn. Reson.* 69, 73–91.
- [33] Mountford, C.E. and Tattersall, M.H.N. (1987) *Cancer Surv.* 6, 285–314.
- [34] May, J.L., Wright, L.C., Holmes, K.T., Williams, P.G., Smith, I.C.P., Wright, P.E., Fox, R.M. and Mountford, C.E. (1986) *J. Biol. Chem.* 261, 3048–3053.
- [35] LeMoyec, L., Tatoud, R., Eugene, M., Gauville, C., Primot, I., Charlemagne, D. and Calvo, F. (1992) *Br. J. Cancer* 66, 626–628.
- [36] Hakumäki, J.M. and Kauppinen, R.A. (2000) *Trends Biochem. Sci.* 25, 357–362.
- [37] Dang, C.V. and Semenza, G.L. (1999) *Trends Biochem. Sci.* 24, 68–72.
- [38] Nelson, B.D. and Kabir, F. (1986) *Biochimie* 68, 407–415.